

## Supplementary Materials for

### **BMP4 preserves the developmental potential of mESCs through *Ube2s*- and *Chmp4b*-mediated chromosomal stability safeguarding**

Mingzhu Wang<sup>1,2,\*</sup>, Kun Zhao<sup>1,2,\*</sup>, Meng Liu<sup>1,2,3,\*</sup>, Mengting Wang<sup>1,2</sup>, Zhibin Qiao<sup>1,2,4</sup>, Shanru Yi<sup>1,2</sup>, Yonghua Jiang<sup>5</sup>, Xiaochen Kou<sup>1,2</sup>, Yanhong Zhao<sup>1,2</sup>, Jiqing Yin<sup>1,2</sup>, Tianming Li<sup>1,2</sup>, Hong Wang<sup>1</sup>, Cizhong Jiang<sup>2,3,†</sup>, Shaorong Gao<sup>1,2,4,†</sup>, Jiayu Chen<sup>1,2,†</sup>.

### Supplementary Figure legends

#### **Fig. S1. S/2i-mESCs present a better developmental potential compared to N/2i-mESCs, Related to Fig. 1.**

- (A) Comparison of the cell cycle of mESCs cultured under S, N/2i and S/2i conditions for 15 days as analyzed by EdU assay. Note that N/2i-mESCs presented an abnormal cell cycle. Data were analyzed from three male mESC lines (#S2, #S3 and #S7).
- (B) Karyotype analysis and representative images of S-, N/2i- and S/2i-mESCs.
- (C) Karyotype analysis of mESCs (#S7) cultured under S, N/2i and S/2i conditions for 15 and 30 days. Data at day 30 were used to assess the significance. n=2 biological replicates.
- (D) Schematic diagram of FACS based chimeric potency assay for accurately determining the *in vivo* differentiation potential of mESCs. Samples include skin, gonads, and other organs of the E13.5 chimeric embryos can be detected.
- (E) Representative flow cytometry images indicate the proportion of mCherry+ cells in skin and Oct4-EGFP+ cells in gonad of E13.5 chimeric embryos.
- (F) Schematic diagram showing the procedure of classical chimera assay and the time required.
- (G) Left, representative images of the gonad (blue dotted line) and mesonephros (red dotted line) of a male and a female E13.5 homozygous OG2-transgenic mouse embryo. Scale bars, 2 mm. Right, histogram showing the percentage of Oct4-EGFP+ cells in the gonad of E13.5 OG2-transgenic embryos. Data are

shown as mean  $\pm$  SEM and analyzed by 11 embryos.

- (H) Resorption statistics of S-, N/2i- and S/2i-mESCs in chimera assay. Note that all N/2i-mESCs showed an obviously high resorption rate in chimera assay. Data were calculated from three male mESC lines (#S2, #S3 and #S7).
- (I) Confirmation of the indicated all-ESC mice by simple sequence length polymorphism (SSLP) assay. Genomic DNA of C57 and 129 mice were used as positive controls and genomic DNA of DBA/2 mice was used as a negative control.

Data are represented as the mean  $\pm$  SEM in (A), (G) and (H), the mean  $\pm$  SD in (C). Statistical analysis was performed using a two-tailed unpaired Welch's t-test. \* $p < 0.05$ ; \*\* $p < 0.01$ ; \*\*\*  $p < 0.001$ .

**Fig. S2. Inactivated TGF $\beta$ , BMP, AKT signaling pathways are improved in S/2i condition, Related to Fig. 2.**

- (A) Volcano Plot showing the global differential expression genes (DEGs) between female N/2i- and S/2i-mESCs. Vertical line indicates expression fold change=2, and horizontal line indicates p-value = 0.01.
- (B) Heatmap showing the expression pattern of stem cell population maintenance genes (171) in N/2i-mESCs was consistently different from that in S- and S/2i-mESCs. Two male cell lines of each condition were used in this test. Each column represents the means of 2-3 biological replicates. Gene lists are described from Mouse Genome Informatics (MGI), GO:0019827.
- (C) Representative house-keeping genes dysregulated in N/2i-mESCs. Dotted line indicates fold change= $\pm 2$ .
- (D) 5-EU incorporation assay indicated an obvious loss of nascent RNA synthesis in N/2i-mESCs compared with S- and S/2i-mESCs. Representative immunofluorescence images of indicated mESCs are shown in the left. Scale bars, 20 $\mu$ m. More than 40 cells were counted for each group. Data are represented as the mean  $\pm$  SEM. Statistical analysis was performed using a two-tailed unpaired Welch's t-test. \*\*\*  $p < 0.001$ .

- (E) GSEA showing the global upregulation of genes related to EGF receptor signaling pathway (n=104), FGF receptor signaling pathway (n=78), HGF receptor signaling pathway (n=13) and Activin receptor signaling pathway (n=45) in S/2i-mESCs compared to N/2i-mESCs. These gene sets were generated by Gene Ontology Browser on MGI website ([http://www.informatics.jax.org/vocab/gene\\_ontology](http://www.informatics.jax.org/vocab/gene_ontology)). NES, normalized Enrichment Score.
- (F) Western blot of SMAD5 and p-SMAD5 in mESC line #S2 under indicated culture conditions. The result showed that BMP4 and serum could promote the phosphorylation level of SMAD5.
- (G) Genome browser view of Smad1/5 binding sites (shaded in grey) at indicated genome loci of representative Klf family members. ChIP-seq data of Smad1/5 in serum/LIF (Serum) and N2B27/LIF+BMP4 (BMP4) mESCs are cited from Morikawa (Morikawa et al., 2016).

**Fig. S3. BMP4 safeguards chromosomal integrity and preserves the developmental potential of mESCs, Related to Fig. 3.**

- (A) Karyotype analysis of mESCs (line #S7) cultured in N/2i and N/2i+BMP4 conditions with or without feeder for 15 and 30 days. Data at day 30 was used to assess the significance. n=2 biological replicates.
- (B) Representative G-banding karyotyping of male mESC line #S2 and #S3 under N/2i+BMP4 condition at day 30.
- (C) The level of H2A.X phosphorylation ( $\gamma$ H2A.X) was higher in N/2i-mESCs compared to N/2i+BMP4-mESCs. Represent images of mESC line #S2 are shown in the right. Scale bars, 20  $\mu$ m.
- (D) Representative morphological images of mESCs cultured under indicated conditions. The pictures were taken at 54 hours after propagation of  $10^5$  cells. Scale bars, 100  $\mu$ m.
- (E) Cell cycle comparison of mESCs cultured under indicated condition for 15 days as analyzed by EdU assay. Note that BMP4 supplemented in N/2i condition could

maintain a regular cell cycle similar to that in serum condition. Three male mESC lines (#S2, #S3 and #S7) were used in this test.

(F) Violin plot showing cell cycle duration of mESCs cultured under indicated conditions. Three male mESC lines (#S2, #S3 and #S7) were used in this test.

(G) Resorption statistics of N/2i- and N/2i+BMP4-mESCs in chimera assay. Note that BMP4 addition greatly reduced the high resorption rate noticed in N/2i-mESCs. Data were calculated from three male mESC lines (#S2, #S3 and #S7).

Data are represented as the mean  $\pm$  SEM in (A), (C), (E)-(G). Statistical analysis was performed using a two-tailed unpaired Welch's *t*-test in (A), (C), (F), (G) and a two-tailed unpaired Student's *t*-test in (E). \**p* < 0.05; \*\**p* < 0.01; \*\*\* *p* < 0.001. n.s., not significant.

**Fig. S4. *Ube2s* and *Chmp4b* are essential for BMP4-mediated chromosomal integrity safeguarding and pluripotency maintenance, Related to Fig. 4.**

(A) RT-qPCR analysis of indicated cell cycle related genes in S-, S/2i-, N/2i- and N/2i+Bmp4-mESCs. *Hprt* was set as an endogenous control. Three male mESC lines (#S2, #S3, and #S7) were tested with 3 biological replicates.

(B) Genome browser view of *Zbtb7a* binding sites (shaded in orange) at *Ube2s* and *Chmp4b* genome loci. ChIP-seq data of *Zbtb7a* in N/2i-mESCs was cited from GSE146653 (Yu et al., 2020).

(C) Validation of indicated gene expressions in control and *Zbtb7a*-overexpressed (OE-*Zbtb7a*) mESCs under N/2i condition. A male mESC line #S2 was used in this test. *Hprt* was set as the endogenous control. *n* = 3 replicates. Data are represented as the mean  $\pm$  SEM. Statistical analysis was performed using a two-tailed unpaired Welch's *t*-test. \**p* < 0.05; \*\*\* *p* < 0.001.

(D) ChIP-qPCR analysis of indicated histone modifications occupancy at promoter regions of *Ube2s* and *Chmp4b* in N/2i- and N/2i+BMP4-mESCs. Two and one potential regulator regions of *Ube2s* and *Chmp4b* were detected, respectively. Relative enrichment was normalized to IgG ChIP signals at the same regions. A male mESC line #S2 was tested with 2 independent experiments. Data are

represented as the mean  $\pm$  SEM. Statistical analysis was performed using a two-tailed unpaired Welch's t-test. \* $p < 0.05$ .

**Fig. S5. *Ube2s* and *Chmp4b* are essential for BMP4-mediated chromosomal integrity safeguarding and pluripotency maintenance, Related to Fig. 4.**

- (A) Validation of knockdown efficiency in sh*Ube2s*- and sh*Chmp4b*-mESCs based on consistent (upper) and inducible gene knockdown (lower) system. shRNA-mESCs were generated from line #S2 and cultured in N/2i+BMP4 condition. The scramble shRNA transfected mESCs were set as the control. As for the inducible system, Dox induction was also conducted in control mESCs. *Hprt* was set as an endogenous control.  $n = 3$  replicates.
- (B) Representative images of control-, sh*Chmp4b*- and sh*Ube2s*-mESCs after propagation under N/2i+BMP4 condition. The sh*Ube2s*-mESCs showed obvious smaller colonies as compared to control- and sh*Chmp4b*-mESCs. The pictures were taken at 54 hours after propagation of  $10^5$  cells. Scale bars, 100  $\mu\text{m}$ .
- (C) Comparison of cell cycle among indicated mESCs as analyzed by EdU assay. Knockdown of *Ube2s* caused a prolongation of the G1 and G2/M phases.  $n = 3$  replicates.
- (D) Validation of cell cycle duration in control-, sh*Chmp4b*- and sh*Ube2s*-mESCs.  $n = 3$  replicates.
- (E) Western blot showing an increased  $\gamma\text{H2A.X}$  level in N/2i+BMP4-mESCs after knockdown of *Ube2s* or *Chmp4b* in mESCs.
- (F) Representative immunofluorescence images of  $\gamma\text{H2A.X}$  enrichment in sh*Ube2s*- and sh*Chmp4b*-mESCs related to Fig. 4F. Scale bars, 20  $\mu\text{m}$ .
- (G) Western blot validated the decrease of *Ube2s* and *Chmp4b* protein levels in mESC line #S2 in inducible gene knockdown system. The scramble ishRNA transfected mESCs after Dox induction was set as the control. KD, knockdown.
- (H) Induced knockdown of *Ube2s* or *Chmp4b* in mESC line #S2 for 5 passages caused an increased resorption rate in chimera assay. The control-, ish*Ube2s*- and ish*Chmp4b*-mESCs were cultured under N/2i+BMP4 condition with Dox for 5

passages before microinjection.

- (I) Validation of overexpression of *Ube2s* (left) and *Chmp4b* (right) in N/2i-mESCs. mESC line #S2 was used in this test. *Hprt* was set as an endogenous control. n = 3 replicates.
- (J) Representative colony morphological images of control-, oe*Ube2s*- and oe*Chmp4b*-mESCs under N/2i condition. The pictures were taken at 54 hours after propagation of  $10^5$  cells. oe, overexpression. Scale bars, 100  $\mu$ m.
- (K) Overexpression of *Ube2s* in N/2i-mESCs could decrease the resorption rate compared to control N/2i-mESCs. oe, overexpression.

Data are represented as the mean  $\pm$  SEM in (A), (C), (D) and (I). Statistical analysis was performed using a two-tailed unpaired Welch's t-test. \*p < 0.05; \*\*p < 0.01; \*\*\*p < 0.001. n.s., not significant.

**Fig. S6. BMP4 can restore the dysregulated transcriptome and long-termly preserve the pluripotency of N/2i-mESCs, Related to Fig. 5.**

- (A and B) Representative images of E13.5 chimeric mice generated from mESCs line #S2 cultured under the N/2i+BMP4 (A) and N/2i (B) conditions for 15, 35 and 55 days after transition. Scale bars, 2 mm.
- (C) Hierarchical clustering of gene expression profiles based on Pearson correlation coefficient in indicated mESCs cultured under indicated conditions. Colors from blue to red indicate weak to strong correlation.
- (D) Heatmap showing the expression level of 4 indicated groups of genes (related to Fig. 2C) in mESCs under different culture conditions. Note that BMP4 could restore the expression of most dysregulated genes in N/2i-mESCs, whereas a2i and t2i did not have a similar role.

**Fig. S7. N/2i+BMP4-mESCs exhibit distinct pluripotent features compared with N/a2i- and N/t2i-mESCs, Related to Fig. 6.**

- (A) Representative morphological images of mESCs cultured under N/2i+BMP4,

N/a2i and N/t2i conditions. mESC line #S2 was used in this test. The pictures were taken at 54 hours after propagation of  $10^5$  cells. Scale bars, 100  $\mu\text{m}$ .

- (B) Karyotyping validation of N/2i+BMP4-, N/a2i- and N/t2i-mESCs. mESC line #S2 was used in this test. More than 40 mitosis phases were counted for each group.
- (C) Representative images of karyotype in N/2i+BMP4-, N/a2i- and N/t2i-mESCs. Analysis was done in a male mESC line #S2 under indicated culture conditions.
- (D) Heatmap showing the expression of representative DNA methylation related genes in indicated mESCs. Two male cell lines of each condition were used in this test. Dotted line indicates fold change =  $\pm 3$ .
- (E) Volcano plot showing the DEGs between male N/a2i- mESCs versus N/2i-mESCs. Vertical line indicates expression fold change = 2, and horizontal line indicates p-value = 0.01.
- (F) Volcano plot showing the DEGs between male N/t2i-mESCs versus N/2i-mESCs. Vertical line indicates expression fold change = 2, and horizontal line indicates p-value = 0.01.
- (G) Expression of representative house-keeping genes under indicated culture conditions. Dotted line indicates fold change =  $\pm 2$ .
- (H) 5-EU incorporation assay in mESC line #S2 under indicated conditions. Representative immunofluorescence images (left) and statistical analysis (right) are shown. The result showed a significant increase of nascent RNA synthesis in N/2i+BMP4-mESCs compared with N/2i-, N/a2i-, and N/t2i-mESCs. More than 40 cells were counted for each group. Scale bars, 20  $\mu\text{m}$ .
- (I) Karyotyping validation of S-, N/2i- and N/2i-S-mESCs. N/2i-S means that N/2i-mESCs were switched back to S condition for 15 days' culturing. Note that N/2i-S mESCs showed a high proportion of aneuploidy similar to that of N/2i-mESCs. The mESC line #S2 was used in this test. More than 40 mitoses phases were counted for each group. n=3 biological replicates.

Data are represented as the mean  $\pm$  SEM in (H) and (I). Statistical analysis was performed using a two-tailed unpaired Welch's t-test. \*p < 0.05; \*\*\* p < 0.001, n.s.,

not significant.

## **REFERENCES**

Morikawa, M., Koinuma, D., Mizutani, A., Kawasaki, N., Holmborn, K., Sundqvist, A., Tsutsumi, S., Watabe, T., Aburatani, H., Heldin, C.H., *et al.* (2016). BMP Sustains Embryonic Stem Cell Self-Renewal through Distinct Functions of Different Kruppel-like Factors. *Stem Cell Reports* 6, 64-73.

Yu, S., Zhou, C., Cao, S., He, J., Cai, B., Wu, K., Qin, Y., Huang, X., Xiao, L., Ye, J., *et al.* (2020). BMP4 resets mouse epiblast stem cells to naive pluripotency through ZBTB7A/B-mediated chromatin remodelling. *Nat Cell Biol* 22, 651-662.

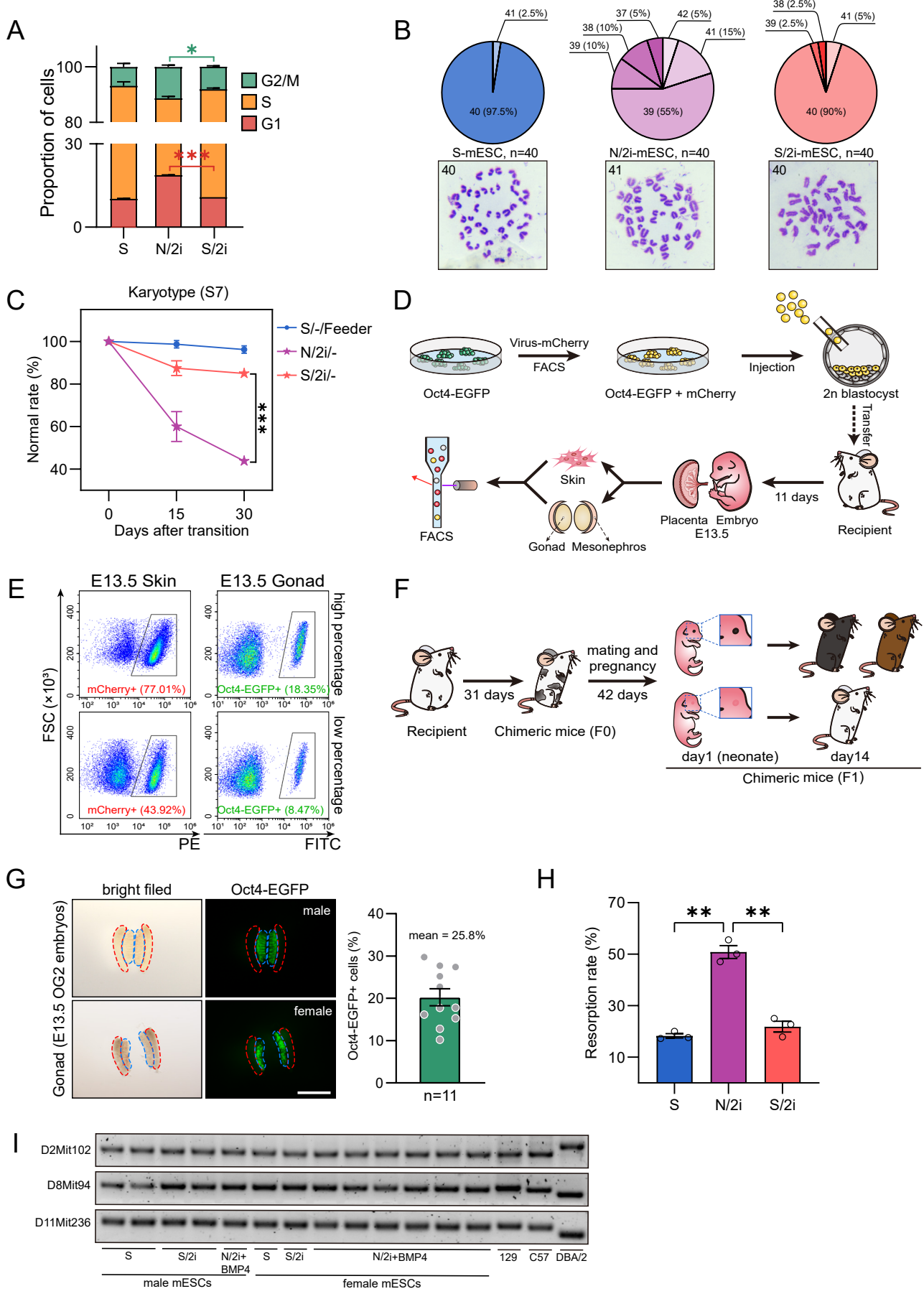


**Figure S1**

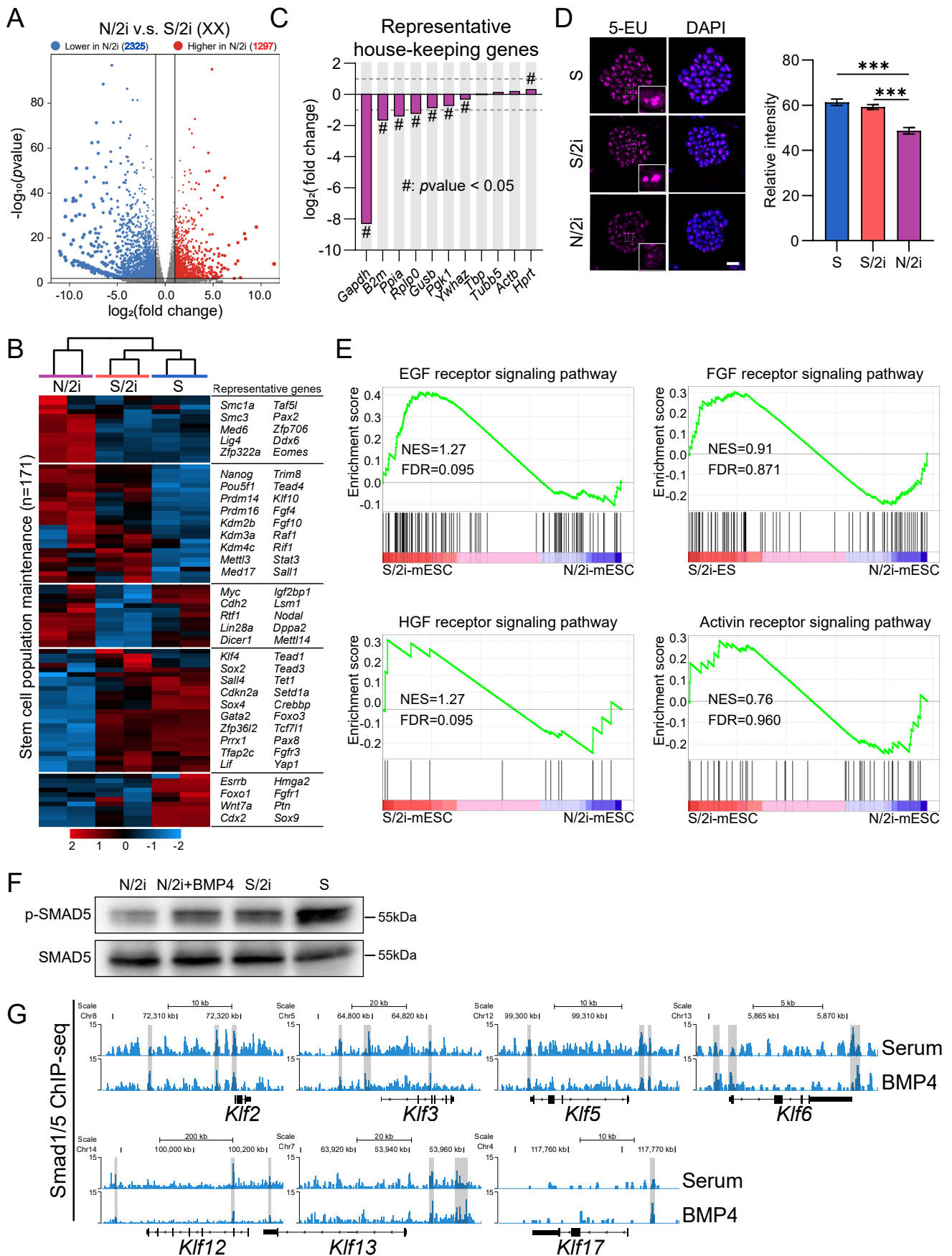


**Figure S2**

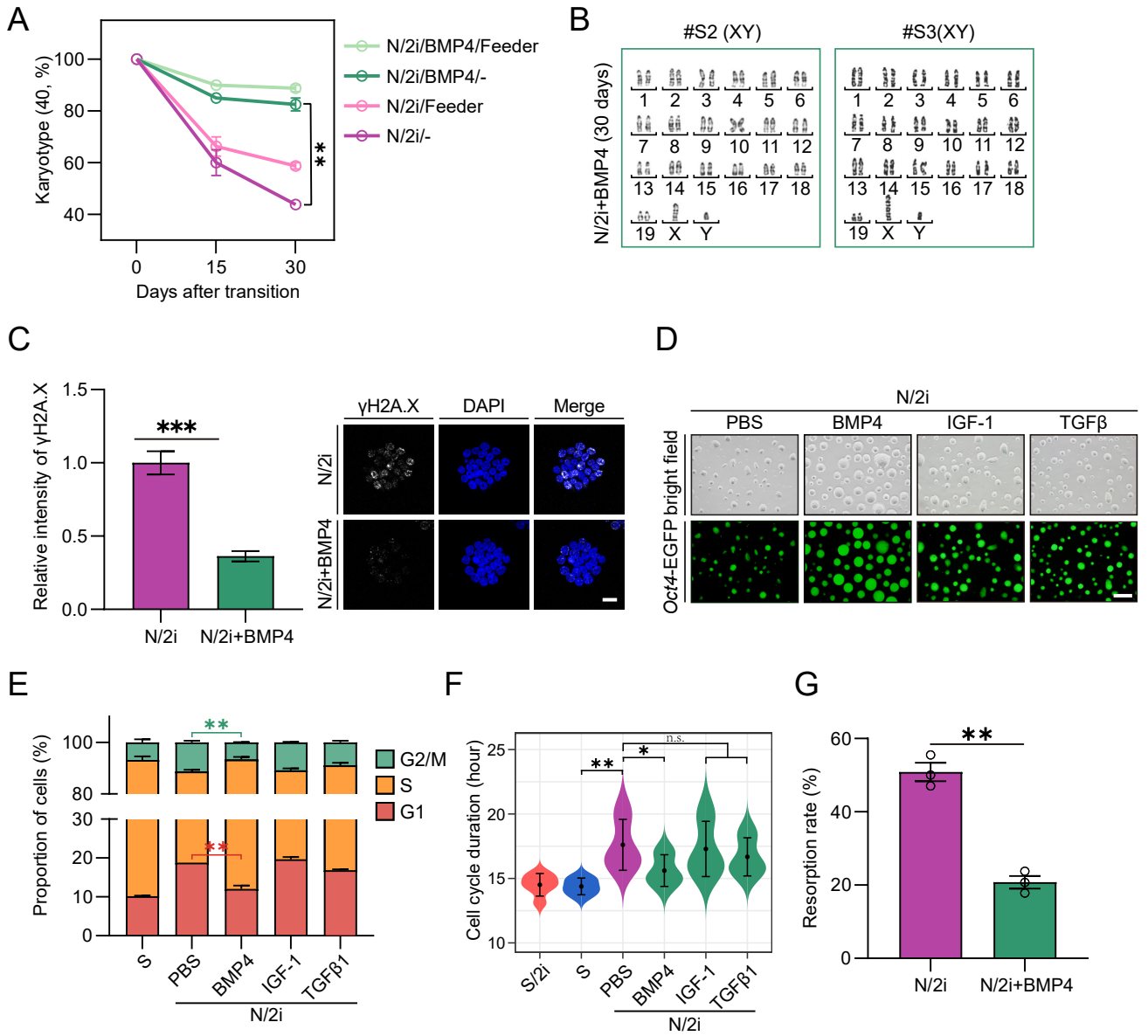


**Figure S3**

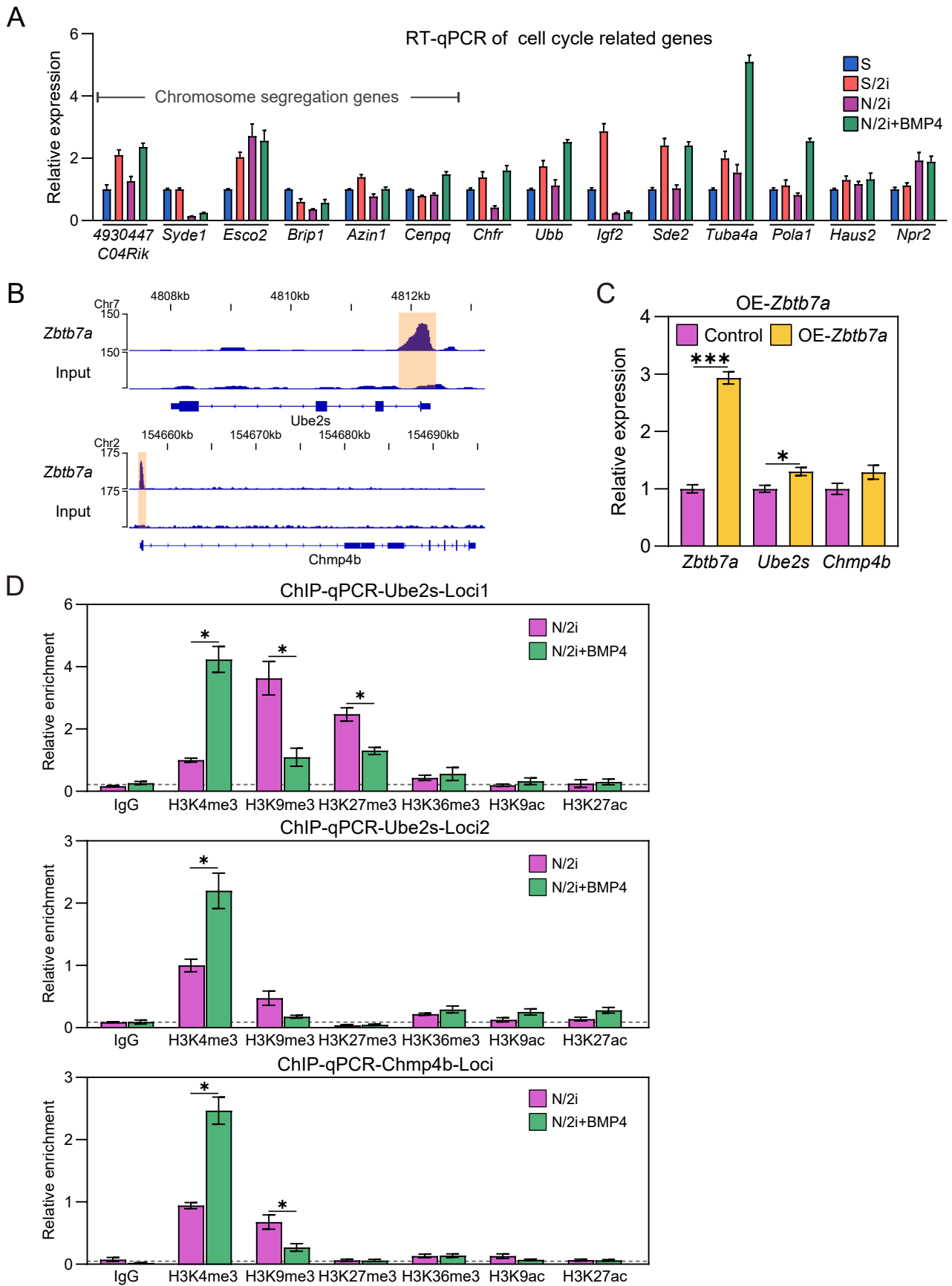


**Figure S4**

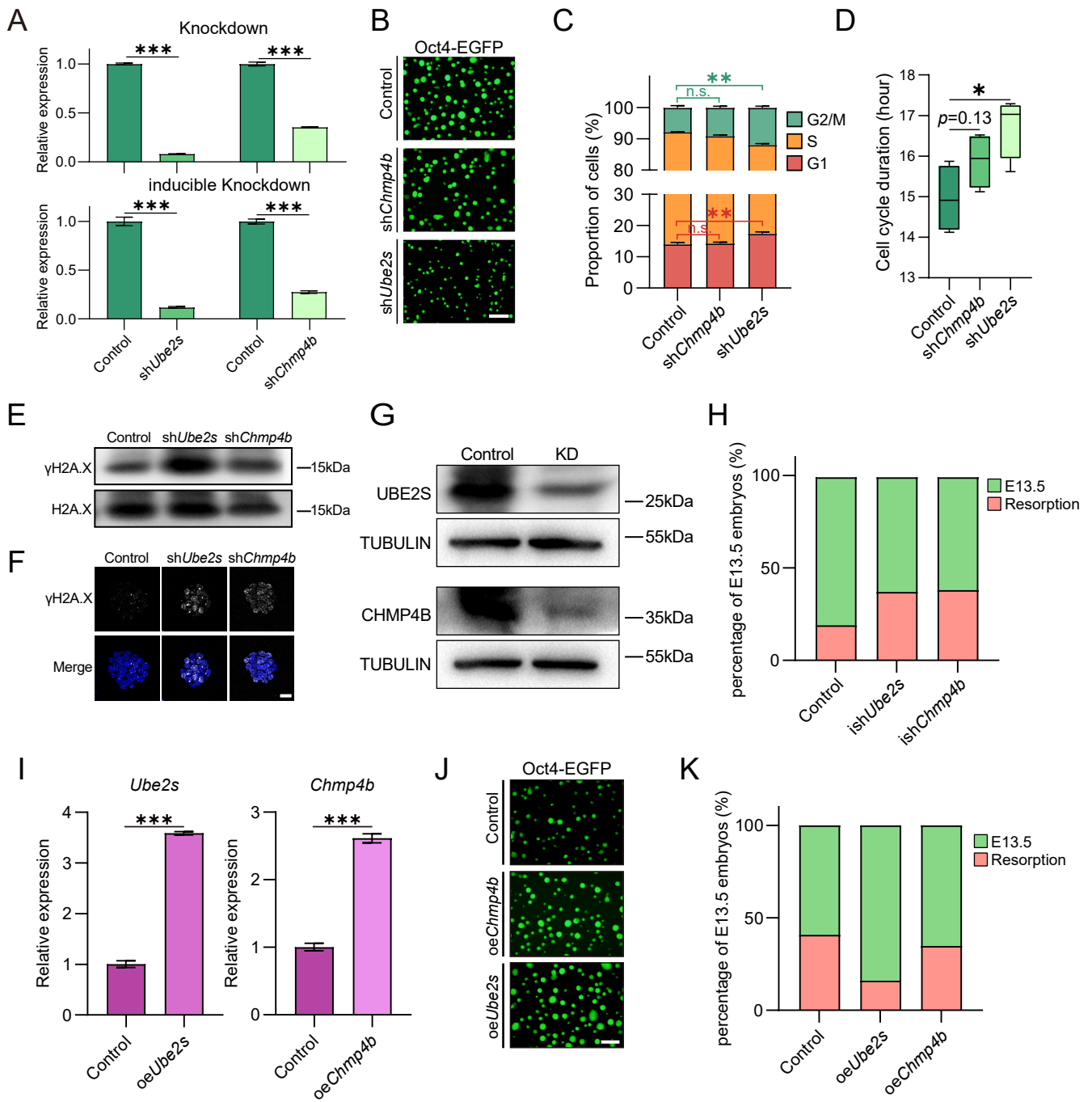


**Figure S5**

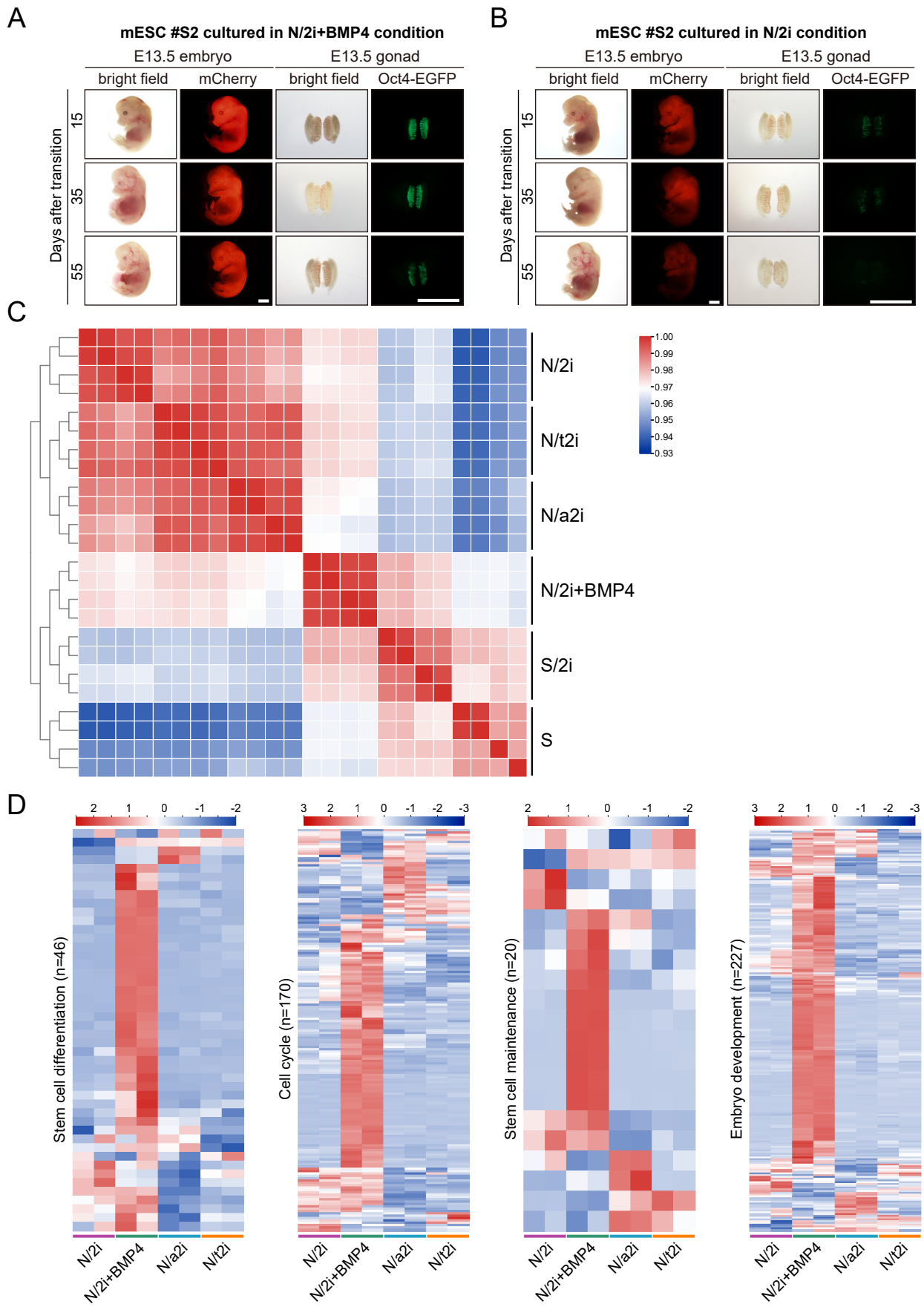


**Figure S6**

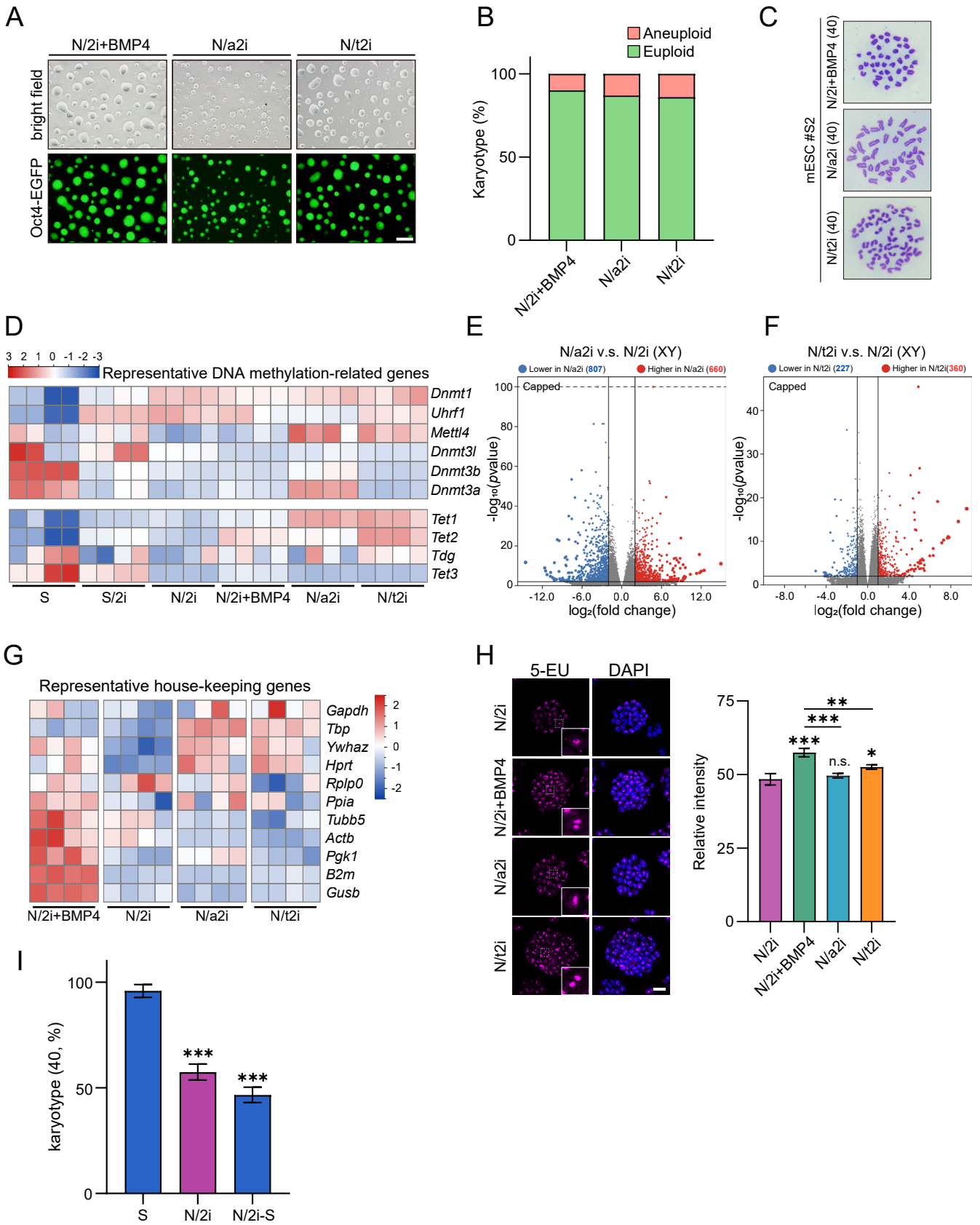


**Figure S7**